Pharmaceutical Research, Vol. 23, No. 6, June 2006 (© 2006)
DOI: 10.1007/s11095-006-0143-7

Research Paper

Reverse Hexagonal Phase Nanodispersion of Monoolein and Oleic Acid for Topical Delivery of Peptides: *in Vitro* and *in Vivo* Skin Penetration of Cyclosporin A

Luciana B. Lopes,[1] Denise A. Ferreira,[1] Daniel de Paula,[1] M. Tereza J. Garcia,[1] José A. Thomazini,[2] Márcia C. A. Fantini,[3] and M. Vitória L. B. Bentley[1,4]

Received November 20, 2005; accepted January 27, 2006

Purpose. To obtain and characterize reverse hexagonal phase nanodispersions of monoolein and oleic acid, and to evaluate the ability of such system to improve the skin penetration of a model peptide (cyclosporin A, CysA) without causing skin irritation.
Methods. The nanodispersion was prepared by mixing monoolein, oleic acid, poloxamer, and water. CysA was added to the lipid mixture to obtain a final concentration of 0.6% (w/w). The nanodispersion was characterized; the skin penetration of CysA was assessed *in vitro* (using porcine ear skin mounted in a Franz diffusion cell) and *in vivo* (using hairless mice).
Results. The obtainment of the hexagonal phase nanodispersion was demonstrated by polarized light microscopy, cryo-TEM and small angle X-ray diffraction. Particle diameter was 181.77 ± 1.08 nm. At 0.6%, CysA did not change the liquid crystalline structure of the particles. The nanodispersion promoted the skin penetration of CysA both *in vitro* and *in vivo*. *In vitro*, the maximal concentrations (after 12 h) of CysA obtained in the stratum corneum (SC) and in the epidermis without stratum corneum (E) + dermis (D) were ~2 fold higher when CysA was incorporated in the nanodispersion than when it was incorporated in the control formulation (olive oil). *In vivo*, 1.5- and 2.8-times higher concentrations were achieved in the SC and [E+D], respectively, when the nanodispersion was employed. No histopathological alterations were observed in the skin of animals treated with the nanodispersion.
Conclusion. These results demonstrate that the hexagonal phase nanodispersion is effective in improving the topical delivery of peptides without causing skin irritation.

KEY WORDS: Cyclosporin A; peptides; reverse hexagonal phase; skin irritation; skin penetration.

INTRODUCTION

The efficacy of dermatological agents is influenced by their penetration within the skin, which can be increased by using adequate topical formulations. Liquid crystalline phases of monoolein (MO), such as reverse hexagonal and cubic phases, present interesting properties for a topical delivery system, and hence have been studied to deliver compounds of pharmaceutical interest to the skin and mucosa (1–3). These phases are (i) bioadhesive, (ii) present a permeation enhancer as the structure forming lipid (MO), and (iii) present ability to incorporate compounds independently of their solubility, to protect them from physical and enzymatic degradation, and to sustain their delivery (2–6). The reverse hexagonal phase (here referred to as hexagonal phase, for simplicity) requires the addition of a third nonpolar compound such as oleic acid to be formed at room temperature (5). Therefore, such a phase also presents the advantage of having two penetrations enhancers in its structure, namely, MO and oleic acid (3,4,7–10).

By modifying the proportions of the components of the bulk hexagonal phase, and by dispersing this liquid crystalline phase in excess water in the presence of a dispersing agent (such as poloxamer), an aqueous dispersion of hexagonal phase particles can be obtained (11–13). It was demonstrated that the dispersed particles retain the internal structure of the bulk phase and its properties (12–17). In comparison with the bulk gel, the dispersion of hexagonal phase presents some advantages. It has a larger surface area to interact with the skin, high fluidity, and can be incorporated into other product formulations (15,16).

Recently, dispersions of cubic phase have been suggested as suitable systems for percutaneous delivery of small molecules such as indomethacin (18). However, the use of other dispersed liquid crystalline phases as colloidal carriers for topical delivery of peptides and proteins has not been explored to date. The present study was aimed at obtaining

[1] Faculdade de Ciências Farmacêuticas de Ribeirão Preto, Universidade de São Paulo, Av. do Café, s/n, Ribeirão Preto, SP 14040-903, Brazil.
[2] Faculdade de Medicina de Ribeirão Preto, Universidade de São Paulo, São Paulo, Brazil.
[3] Instituto de Física, Universidade de São Paulo, São Paulo, Brazil.
[4] To whom correspondence should be addressed. (e-mail: vbentley@usp.br)

and characterizing aqueous dispersions composed of hexagonal phase particles of nanometric size (referred to as nanodispersion in this study) for topical delivery of peptides. Before developing and validating a more complex method to assess the skin penetration of a model peptide in the skin, we probed whether the hexagonal phase nanodispersion had the ability to increase the skin penetration of a small molecule of easy detection, the fluorescent marker fluorescein isothiocyanate (FITC). Having demonstrated the formulation's ability to increase the skin penetration of FITC, we next evaluated whether the skin penetration of a model, a relatively large peptide, could also be increased by its incorporation in the nanodispersion. CysA was chosen as the model peptide due to its poor skin penetration (unless a chemical or physical technique is used) and its usefulness in the treatment of cutaneous diseases (19–21). Lastly, we tested whether the nanodispersion causes skin irritation.

MATERIALS AND METHODS

Materials

Monoolein (MO, Myverol 18-99) was supplied by Quest (Norwich, NY, USA), oleic acid and FITC were obtained from Sigma (St. Louis, MO, USA), poloxamer 407 was obtained from BASF (Florham Park, NJ, USA), and CysA from Boechel (Hamburg, Germany). Acetonitrile and methanol were purchased from Ominsolve (Merck, Darmstadt, Germany).

Preparation of the Hexagonal Phase Nanodispersion

Bulk hexagonal phases containing excess water were prepared by mixing melted monoolein (at 42°C) and oleic acid (8:2 w/w), and by adding a 1% aqueous solution of poloxamer to the lipid mixture to achieve a monoolein/oleic acid/poloxamer/water system (8:2:0.9:89.1, w/w/w/w). The selected monoolein/oleic acid ratio has been shown to lead to the formation of a hexagonal phase gel (5), and the selected poloxamer/lipid ratio has been demonstrated to allow the formation of dispersed hexagonal phase particles (12). The system was allowed to equilibrate at room temperature for 24 h. Then, the hexagonal phase with excess water was vortex-mixed, sonicated in ice-bath for 1 min, and passed through a 0.8-μm membrane. The resulting dispersion had pH of 6.3–6.4. A dispersion containing CysA (model peptide; 0.6% or 4%, w/w) or FITC (fluorescent marker; 0.03%, w/w) was obtained by adding either compound to the initial monoolein–oleic acid mixture.

Characterization of the Hexagonal Phase Dispersions

Polarized Light Microscopy

The MO/oleic acid/poloxamer/water system (8:2:0.9:89.1, w/w/w/w) and the MO/oleic acid/drug/poloxamer/water system [MO/oleic acid/CysA/poloxamer/water at 8:2:0.6:0.9:88.5 (w/w/w/w/w) and MO/oleic acid/FITC/poloxamer/water at 8:2:0.03:0.9:89.07 (w/w/w/w/w)] were characterized under a polarized light microscope (Axioplan 2 Image Pol microscope, Carl Zeiss, Oberkochen, Germany) before and after the sonication process used to disperse the bulk phase.

Small-Angle X-Ray Diffraction

To characterize the liquid crystalline structure of the dispersed particles, small-angle synchrotron radiation X-ray diffraction measurements were performed at the Brazilian Synchrotron Light Laboratory (LNLS), Campinas, SP, Brazil, using the D11A-SAXS beamline (22,23). The white photon beam was extracted from the ring through a high-vacuum path. After passing through a thin beryllium window, the beam was monochromatized and horizontally focused by a cylindrically bent and asymmetrically cut (111) silicon single crystal. The selected wavelength was 1.608 Å. The focus was located at the detection plane. The scattered intensities were collected by a one-dimension position sensitive detector located at 736.5 mm from the sample. An ionization detector monitored the intensity of the incident beam. The data were corrected by detector homogeneity, incident beam intensity, sample absorption, and blank subtraction (poloxamer/water solution). Unloaded nanodispersion and nanodispersions containing 0.6 or 4% (w/w) of CysA were analyzed.

Cryo-Transmission Electron Microscopy

The liquid crystalline structure of the particles of the unloaded nanodispersion and their morphology was also investigated by cryo-transmission electron microscopy (Cryo-TEM). The samples were prepared with slight modifications of the procedures first described by Bellare *et al.* (24). The method consisted of obtaining a thin vitrified aqueous film of the sample in a controlled environment vitrification system (CEVS), where temperature and humidity could be controlled. A drop (~1 μL) of the unloaded nanodispersion was deposited on a copper TEM grid covered with a perforated polymer film and blotted to form a thin film using filter paper. After blotting, the sample was immediately vitrified in liquid ethane held (with liquid nitrogen) at its freezing point. The vitrified sample was then transferred under liquid nitrogen to a Zeiss EM 902A transmission electron microscope (Carl Zeiss NTS, Oberkochen, Germany). The instrument was operating at 80 kV and in zero loss brightfield mode. The specimen temperature was kept below −160°C and protected against atmospheric conditions during examination.

Light Scattering

The mean diameter and particle size distribution of unloaded nanodispersion and the nanodispersion containing CysA at 0.6% (w/w) were determined by using a dynamic light scattering system (Malvern 4700, Malvern, UK) at 90° with a He–Ne laser. Samples were diluted in particle-free purified water, and the measurements ($n = 3$ for each sample) were performed at 25°C.

In Vitro Skin Penetration

Skin Penetration of FITC

As the hexagonal phase dispersion had never been used for topical delivery, we first tried to visualize FITC skin penetration. FITC was chosen as the fluorescent marker because it presents relatively high absorptivity, good fluores-

cence quantum yield, and low cost, and because its extensive use in the past makes it a very well characterized fluorophore for microscopy. The penetration of FITC in the skin was assessed in an *in vitro* model using porcine ear skin (25). The skin from the outer surface of a freshly excised porcine ear was carefully dissected (making sure that the subcutaneous fat was maximally removed), stored at −20°C, and used within a month. On the day of the experiment, the skin was thawed and mounted in a Franz diffusion cell (diffusion area of 1 cm^2; Laboratory Glass Apparatus, Inc., Berkeley, CA, USA), with the stratum corneum facing the donor compartment (where the formulation was applied) and the dermis facing the receptor compartment. The latter compartment was filled with 100 mM phosphate buffer (pH 7.2) containing ethanol (10%), and maintained at 37°C under constant stirring. We chose the receptor phase buffered at 7.2 based on previous published studies that evaluated lipid-based systems (25–28). Previous studies used receptor phases containing up to 20% of ethanol (29). A hundred microliters of an FITC-containing dispersion (0.03% w/w) or a hydroalcoholic (10% ethanol) solution of FITC (0.03% w/w) was applied to the surface of the skin. Because the skin presents autofluorescence, skin sections treated with PBS were used as control.

After 6 h, the surface of the skin was carefully cleaned, and the diffusion area of skin samples was frozen by using isopentane at −30°C, embedded in Tissue-Tek® OCT compound (Pelco International, Redding, CA, USA), and sectioned using a cryostat microtome (Leica, Wetzlar, Germany). The skin sections (8 μm) were mounted on glass slides. The slides were visualized without any additional staining or treatment through a 20× objective using a Zeiss microscope (Carl Zeiss, Thornwood, NY) equipped with a filter for FITC and AxioVision software.

FITC present in the receptor phase was quantified by fluorimetry. Samples (2 mL) of the receptor phase were lyophilized for 24 h, and the residue was dissolved in 200 μL hydroalcoholic (10% ethanol) solution. All solutions were subjected to fluorimetry analysis using a Gemini SpectraMax platereader (Molecular Devices, Sunnyvale, CA, USA) with excitation at 495 nm and emission at 518 nm.

Skin Penetration of CysA

The skin penetration of CysA incorporated in the hexagonal phase nanodispersion was assessed using porcine ear skin mounted in the Franz diffusion cell (diffusion area of 1.77 cm^2; Hanson instruments, Chatsworth, CA, USA). The receptor compartment was filled with 100 mM phosphate buffer (pH 7.2) containing ethanol (10%). The receptor phase was maintained at 37°C and under constant stirring. One hundred milligrams of the nanodispersion containing 0.6% CysA (w/w) was applied to the surface of the stratum corneum. A solution of CysA (0.6%, w/w) in olive oil was used as the control formulation because, being the goal of the present study to evaluate the ability of the nanodispersion as a whole to improve the delivery of CysA to the skin, it was important to use a vehicle that contains no component of the formulation. As in a previous study (19), we used olive oil.

At 6 or 12 h postapplication, skin surfaces were carefully washed with distilled water and wiped with a cotton swab to remove excess formulation. To separate the stratum corneum (SC) from the remaining epidermis (E) and dermis (D), skin sections were subjected to tape stripping (21). The skin was stripped with 15 pieces of adhesive tape, and the tapes containing the SC were immersed in 5 mL methanol and vortex-stirred for 2 min. The methanolic phase was filtered using a 0.45-μm membrane, and the resulting filtrate assayed for CysA. The remaining [E + D] was cut in small pieces, vortex-mixed for 2 min in 2 mL methanol, and bath-sonicated for 30 min. The resulting mixture was filtrated using 0.45-μm membranes, and CysA was assayed in the filtrate. The amounts of drug detected in SC and in [E + D] are indicatives of drug penetration in the skin.

To validate the extraction procedure, the absolute recovery of CysA from skin tissue was determined by spiking skin sections (area of 1.77 cm^2) with CysA solutions in methanol (100 and 200 μg/mL). The spiked skin sections ($n = 5$ for each concentration) were allowed to rest for 20 min, and CysA was extracted as described above from the SC and [E + D]. Recovery of CysA from the skin (SC + [E + D]) was 89 ± 4.9% and 92.5 ± 2.1% for the lower and higher concentrations, respectively.

In Vivo Skin Penetration of CysA

Hairless mice (males, 6–8 weeks old) were obtained from the colony of the Pharmacy School of Ribeirão Preto (University of São Paulo, Ribeirão Preto, SP, Brazil). They were housed at 24–26°C, exposed to a daily 12:12-h light/dark cycle (lights on at 6:00 A.M.), and had free access to standard mice chow and tap water. To reduce the stress associated with the experimental procedure, the mice were handled daily for 1 week before experimentation. The protocols were in accordance with the Principles of Laboratory Animal Care (NIH publication) and with the guidelines of the University of Sao Paulo Animal Care and Use Committee.

On the day of the experiment, 100 mg of CysA-containing nanodispersion or control formulation (CysA in olive oil at 0.6%, w/w) was applied to a limited area (2 cm^2) of the skin on the back of each mouse. At 6 h postapplication, each mouse was killed with an overdose of carbon dioxide, and the skin area where the formulation was applied was dissected. The skin was subjected to tape stripping (as described for the *in vitro* permeation experiment), and the amount of CysA in the SC and [E + D] was determined.

Skin Irritation Test

To evaluate whether the hexagonal phase nanodispersion caused skin irritation, the occurrence of histological changes in the skin of hairless mice was examined after topical application of the system for 2 days. One hundred milligrams of the nanodispersion was applied topically on a limited area (~2 cm^2) (30) of the skin on the back of each mouse once a day for 2 days. On the third day (~12 h after the second application of the formulation), the animals were killed with an overdose of carbon dioxide and the skin area where the formulation was applied was dissected, fixed by immersion in Bouin liquid at room temperature for 24 h, processed for inclusion in paraffin, sectioned with 6 μm of thickness, and stained with Masson tricromic. This regimen was chosen to simulate a short-term treatment. Skin sections

were examined under conventional light microscopy (Carl Zeiss, Oberkochen, Germany) for epidermis thickening, edema, and infiltration of inflammatory cells in the dermis (30). Epidermis thickness was measured using the AxiVision software (Carl Zeiss, Oberkochen, Germany). The skin of untreated animals and animals treated with saline were used as the controls. In another study conducted in our laboratory (Lopes *et al*., unpublished data), this method was found to be sensitive enough to detect skin irritation caused by a bulk hexagonal phase gel.

Analytical Methodology for CysA

CysA was assayed by high-performance liquid chromatography (HPLC) using a Shimadzu equipment, which consisted of a Model LC10 AD solvent pump, a Rheodyne injector, a 20-μL loop, a Model SPD-10A variable wavelength UV detector, a Model CTO-10A column oven, and a Model SCL-10A controller system. The separation was performed by a Lichrospher 100 RP-18 column (5 μm; Merck), which was equipped with a RP-8 precolumn (Merck) and equilibrated at

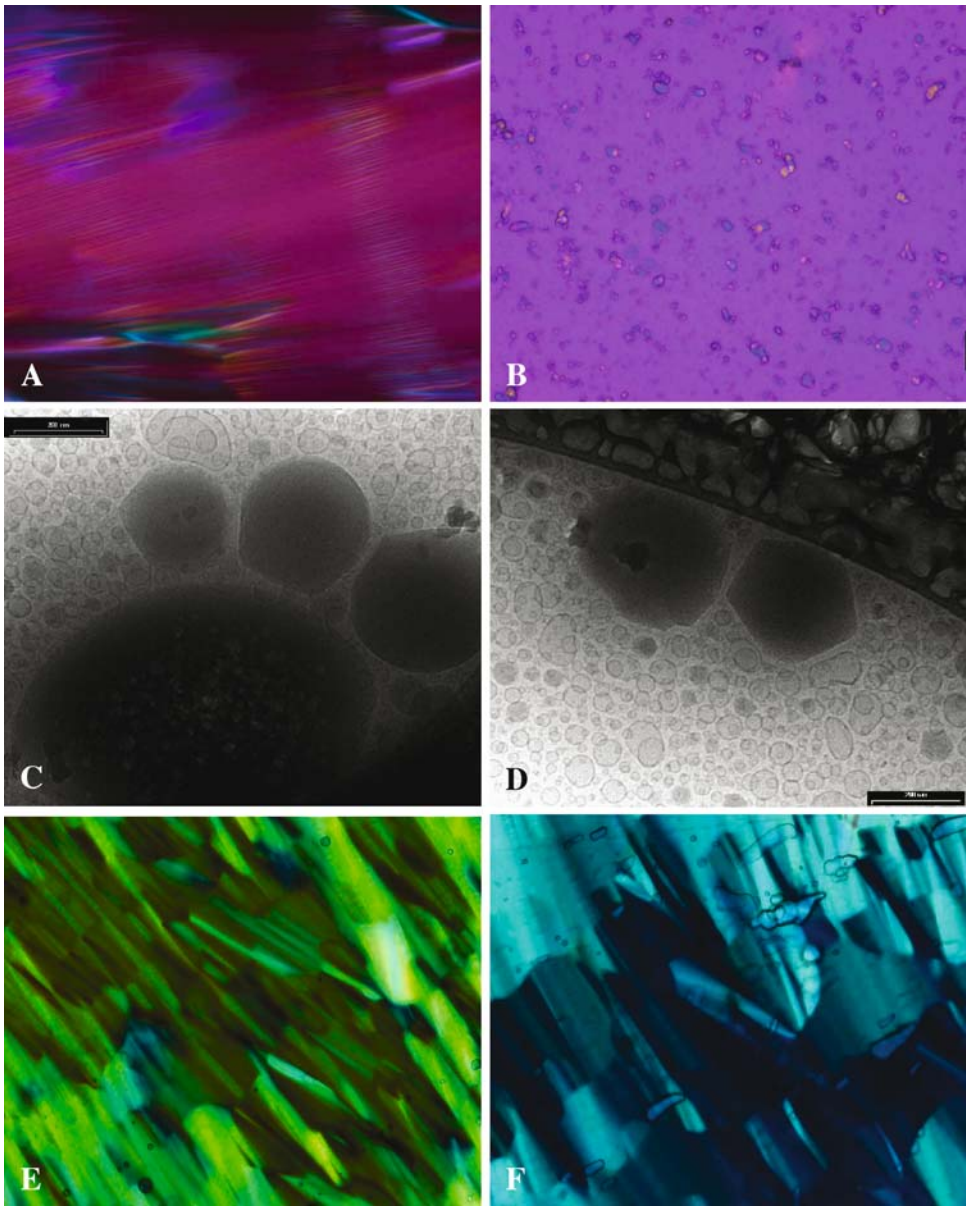

Fig. 1. Microscopic characterization of the bulk hexagonal phase and hexagonal phase nanodispersion. (A) Polarized light microscopy of the bulk hexagonal phase composed of monoolein/oleic acid/poloxamer/water at 64:16:0.9:19.1 (w/w/w/w). (B) Polarized light microscopy of the hexagonal phase nanodispersion composed of monoolein/oleic acid/poloxamer/water at 8:2:0.9:89.1 (w/w/w/w). (C and D) Cryo-TEM microscopy of the hexagonal phase nanodispersion (scale bar: 200 nm). (E) Polarized light microscopy of the bulk hexagonal phase with excess water composed of MO/oleic acid/FITC/poloxamer/water at 8:2:0.03:0.9:89.07 (w/w/w/w/w). (F) Polarized light microscopy of the bulk hexagonal phase with excess water composed of MO/oleic acid/CysA/poloxamer/water at 8:2:0.6:0.9:88.5 (w/w/w/w/w).

60°C. A mobile phase of 67% acetonitrile and 33% water (flow rate of 1 mL/min) was used, and CysA was detected at 210 nm. Under these conditions, the retention time of CysA was 9.1 min. The area under the peak was used to calculate the concentration range of CysA and linearity was achieved over the concentration range between 0.15 and 500.00 μg/mL, presenting a following correlation coefficient (r) of 0.9998. The detection sensibility of this HPLC assay was 0.15 μg/mL, with less than 5.15% intraday variation, and less than 2.77% interday variation. The error was less than 5.50%. Using this HLPC procedure, unidentified peaks were not detected.

Statistical Analyses

The results are reported as means ± SD. As in previous skin penetration studies (21), data were statistically analyzed using nonparametric tests. Mann-Whitney test was used to compare two experimental groups. Kruskal-Wallis test (followed by Dunns *post-hoc* test) was used to compare more than two experimental groups. The level of significance was set at $p < 0.05$.

RESULTS

Characterization of the Hexagonal Phase Dispersions

Unloaded Nanodispersion

The liquid crystalline structure of the nanodispersion composed of MO, oleic acid, poloxamer, and water was characterized by polarized microscopy, Cryo-TEM, and small angle X-ray diffraction (SAXRD). The system composed by MO/oleic acid/poloxamer/water at 64:16:0.9:19.1 (w/w/w/w) presented a fanlike structure, typical of hexagonal phase, as observed by polarized light microscopy (Fig. 1A). The addition of excess water in the system (MO/oleic acid/poloxamer/water at 8:2:0.9:89.1, w/w/w/w) led to the obtainment of a mixture of hexagonal phase plus excess water. The sonication of such a system resulted in the obtainment of a milky, low-viscosity, and anisotropic dispersion, which was passed through a 0.8-μm membrane to obtain particles with similar size (Fig. 1B).

The shape and structure of the particles were investigated by Cryo-TEM, and we observed that the sonication of the MO/oleic acid/poloxamer/water system (8:2:0.9:89.1, w/w/w/w) gave rise to more or less faceted particles, many of which showed textures of hexagonal symmetry (Fig. 1C and D). These particles were observed together with some vesicular structures, which have already been observed by other authors, especially when sonication was used to disperse the hexagonal phase in water (12,16).

The internal structure of the particles was further investigated by SAXRD. Dispersed samples gave broad X-ray reflections, which is probably a consequence of the small crystallite sizes (Fig. 2). The X-ray diffractograms of the unloaded nanodispersion displayed three to four diffraction lines. The diffraction lines were indexed, and the hexagonal structure of the formed phase was demonstrated (Fig. 2 and Table I). This is in accordance with the cryo-TEM observations. The particle diameter of the unloaded nanodispersion was 181.77 ± 1.08 nm.

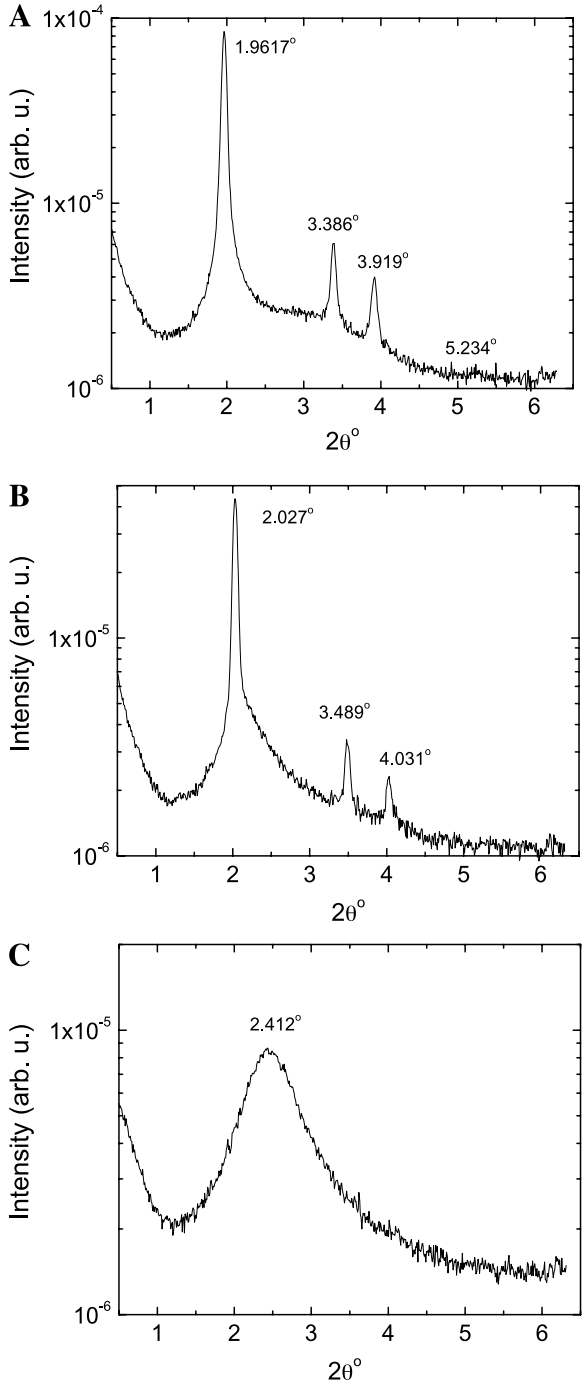

Fig. 2. Small-angle X-ray diffraction patterns of the unloaded hexagonal phase nanodispersion (A), nanodispersion containing 0.6% of CysA (B), and nanodispersion containing 4% of CysA (C).

Dispersion Containing FITC

Addition of FITC (0.03%, w/w) to the MO/oleic acid system allowed the obtainment of the bulk hexagonal phase with and without excess water, as observed by polarized light microscopy. The system showed a fanlike texture, typical of the hexagonal phase (Fig. 1E). After sonication of the bulk phase with excess water and filtration of the resulting system,

Table I. Small-Angle X-ray Diffraction Data for the Dispersions

Sample	2θ (deg)	d (Å)	Ratio and (hkl)	Structure
Unloaded nanodispersion	1.962	45.03	1/1 (100)	Hexagonal
	3.386	26.09	1/√3 (110)	Hexagonal
	3.919	22.55	1/√4 (200)	Hexagonal
	5.234	16.88	1/√7 (210)	Hexagonal
Nanodispersion + 0.6% CysA	2.027	43.58	1/1 (100)	Hexagonal
	3.489	25.32	1/√3 (110)	Hexagonal
	4.031	21.92	1/√4 (200)	Hexagonal
	–	–	1/√7 (210)	Hexagonal
Nanodispersion + 4% CysA	2.412	36.62	–	–

Samples: unloaded hexagonal phase nanodispersion, nanodispersion containing 0.6% of CysA, and nanodispersion containing 4% of CysA. θ = diffraction angle, d = observing Bragg spacing, hkl = Miller indices.

a milky, low-viscosity, and anisotropic dispersion (like the unloaded system) was obtained.

Dispersion Containing CysA

Addition of CysA (0.6%, w/w) to the MO/oleic acid system also allowed the obtainment of the hexagonal phase with and without excess water (Fig. 1F). The internal structure of liquid crystalline nanodispersion was unaltered by 0.6% CysA, as demonstrated by SAXRD (Table I and Fig. 2). The X-ray diffractogram of the nanodispersion containing 0.6% CysA displayed three diffraction lines; the lines were indexed, and the results demonstrated the hexagonal structure. On the other hand, 4% CysA disorganized the system, and a hexagonal structure was no longer observed. Samples of the bulk phase containing excess water (more than 85%) and 4% CysA did not exhibit textures of hexagonal phase, as observed by polarized light microscopy. The X-ray diffractogram of the nanodipersion containing CysA at 4% presented only one broad reflection, and the internal structure of the particles could not be determined (Table I and Fig. 2). Because CysA at 4% did not allow the formation of the hexagonal phase nanodispersion, this concentration was not used for further experiments.

The presence of CysA at 0.6% slightly decreased the size of the particles (diameter of 162.62 ± 1.04 nm). The polydispersity index was below 0.150–0.200. Because light scattering analysis demonstrated the presence of particles of nanometric size, the system was referred to as nanodispersion.

In Vitro Skin Penetration

Skin Penetration of FITC

The skin penetration of FITC incorporated in the MO/oleic acid dispersion or in a hydroalcoholic solution was visualized by fluorescence microscopy. As expected (31),

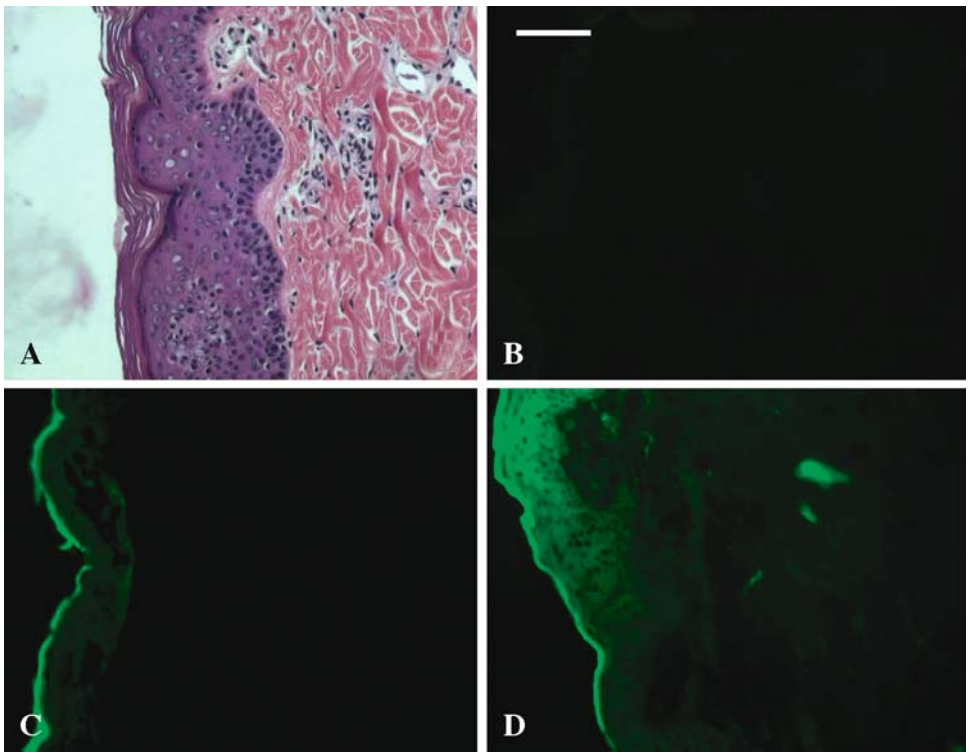

Fig. 3. Microscopic evaluation of porcine ear skin after treatment for 6 h with different formulations. (A) Light microscopy of skin treated with PBS (hematoxylin staining). (B) Fluorescence microscopy of skin section treated with PBS. (C) Fluorescence microscopy of skin treated with the hidroalcoholic solution of FITC. (D) Fluorescence microscopy of skin treated with the nanodispersion containing FITC. Sections were visualized using FITC filter through a 20× objective. Scale bar: 100 μm. Three batches of each formulation were tested, and representative pictures are shown.

untreated skin presented a very weak autofluorescence (especially the SC; Fig. 3A and B). When FITC was incorporated in the hydroalcoholic solution, fluorescence was predominantly present in the SC, and only a weak fluorescence was observed in the epidermis (Fig. 3C). On the other hand, treatment of the skin with the MO/oleic acid dispersion containing FITC resulted in a strong fluorescent staining of SC and viable epidermis (Fig. 3D). Some fluorescence could also be observed in the dermis. No FITC was detected at 6 h postapplication in the receptor phase using either the hydroalcoholic solution or the nanodispersion.

Skin Penetration of CysA

We next evaluated the ability of the hexagonal phase nanodispersion to increase the skin penetration of a model peptide *in vitro*. Compared to the control formulation (olive oil), the nanodispersion significantly enhanced the skin penetration of CysA (Fig. 4). When CysA was incorporated in the nanodispersion, its concentration in the SC was significantly enhanced at 6 h ($p < 0.05$) and 12 h ($p < 0.01$) postapplication. Similarly, CysA concentration in [E + D] was significantly enhanced after 6 and 12 h ($p < 0.05$). When the control formulation was used, the maximal concentrations of CysA were achieved at 12 h postapplication. We found that 6.51 ± 1.42% of the applied dose/cm^2 of CysA was delivered to the SC, whereas 2.48 ± 0.53% of the applied dose/cm^2 of CysA was delivered to [E + D]. Using the hexagonal phase nanodispersion, the maximal concentrations of CysA in the SC and [E + D] were ~2-fold higher than those obtained when CysA was incorporated in the control formulation. On the other hand, no CysA was detected in the receptor phase after 12 h using either the control formulation or the nanodispersion.

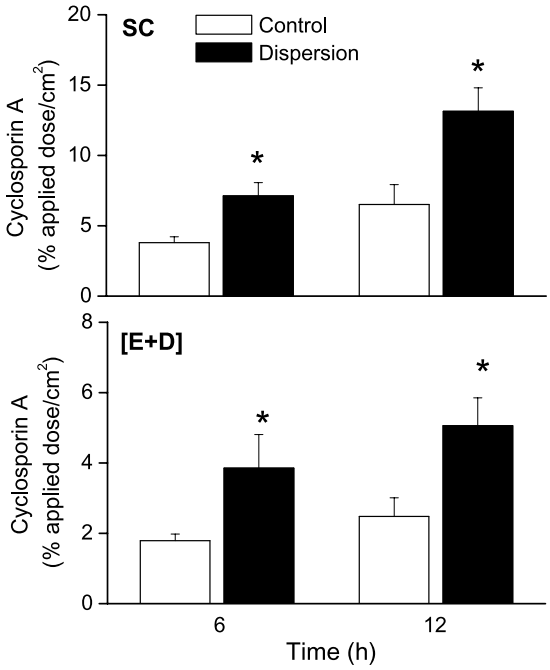

Fig. 4. *In vitro* penetration of CysA in the SC and [E + D] at 6 and 12 h following its topical application using the hexagonal phase nanodispersion or the control formulation. SC: stratum corneum, [E + D]: epidermis (without SC) plus dermis, * $p < 0.05$. Five to six batches of each formulation were tested, and the results are shown as mean ± SD.

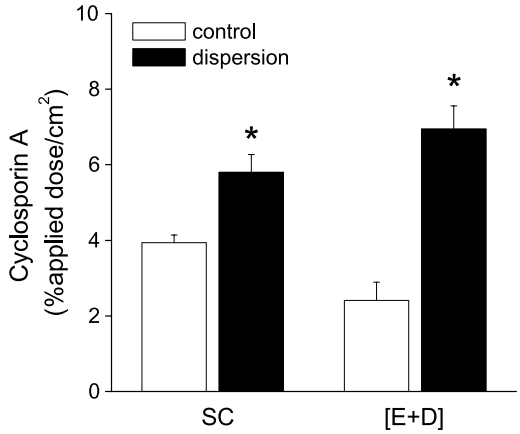

Fig. 5. *In vivo* skin penetration of CysA at 6 h following its topical application using the hexagonal phase nanodispersion or the control formulation. SC: stratum corneum, [E + D]: epidermis (without SC) plus dermis, * $p < 0.05$. Four to five batches of each formulation were tested, and the results are shown as mean ± SD.

In Vivo Skin Penetration of CysA

In vivo penetration of CysA in the SC and [E + D] was evaluated using hairless mice. Similar to our *in vitro* observations, the hexagonal phase nanodispersion significantly ($p < 0.05$) enhanced the skin penetration of CysA *in vivo* at 6 h postapplication compared with the control formulation (Fig. 5). When CysA was incorporated in the control formulation, ~3.91 ± 0.20% and 2.41 ± 0.48% of the applied dose/cm^2 was detected in SC and [E + D], respectively, at 6 h postapplication. When CysA was incorporated in the nanodispersion, 1.5 and 2.8 times higher concentrations were achieved in the SC and [E + D], respectively.

Skin Irritation Test

On the third day after topical application of the nanodispersion or an inert solution (saline), the histological characteristics of the skin were determined. We searched for three established endpoints of irritation: epidermal thickening, edema, and immunocyte infiltration in dermis. Light microscopy indicated none of these endpoints in the skin of animals treated with the hexagonal phase nanodispersion or saline, as compared to the untreated animals (Fig. 6A–C). Figure 6D shows the thickness of epidermis of animals subjected to topical treatment with saline or with the unloaded nanodispersion; no significant difference was observed in comparing the nanodispersion-treated, saline-treated, and untreated animals.

DISCUSSION

Aqueous dispersions of liquid crystalline phases of MO have been previously obtained and characterized (11,12,16,32,33), but the use of hexagonal phase dispersions as colloidal carriers for topical delivery of peptides and

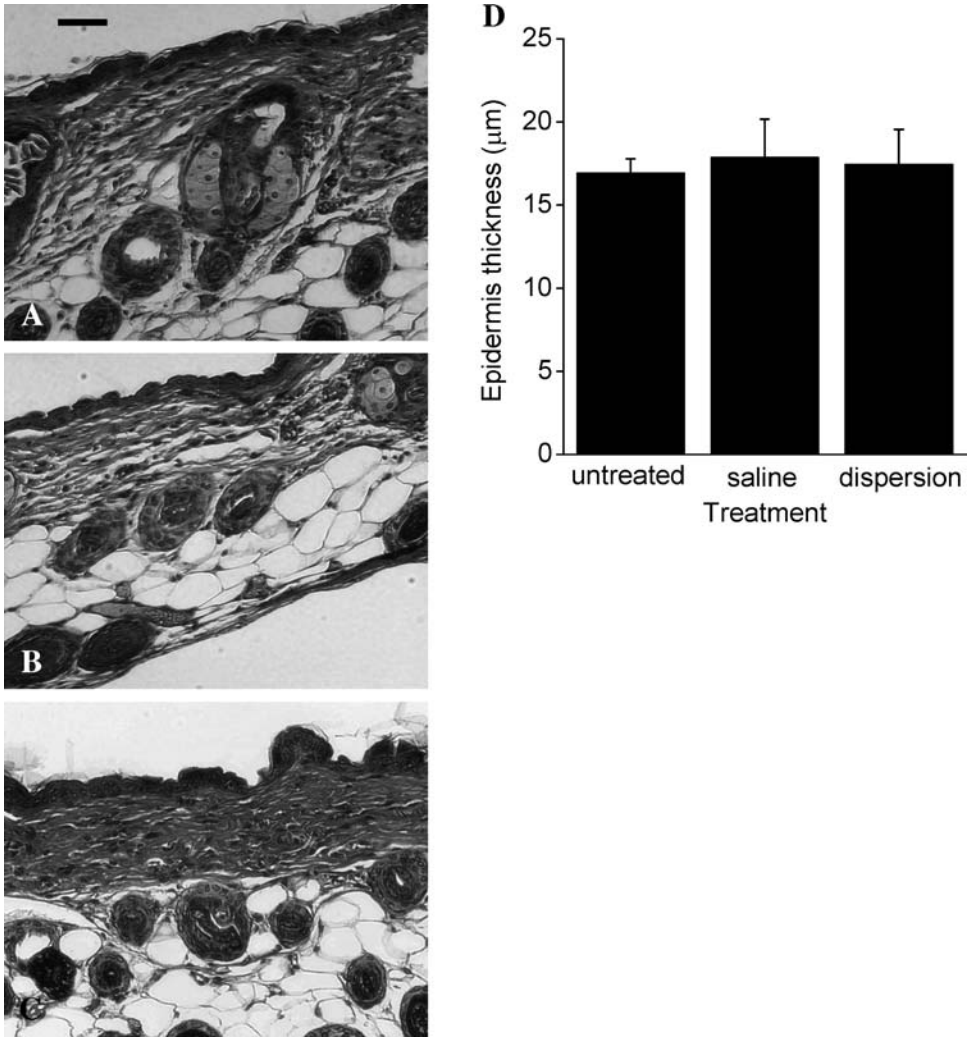

Fig. 6. Analysis of the skin of untreated animals and animals subjected to topical application of saline or nanodispersion. (A) Light microscopy of untreated skin. (B) Light microscopy of skin treated with PBS. (C) Light microscopy of skin treated with the hexagonal phase nanodispersion. (D) Thickness of the epidermis of untreated animals and those treated with saline or nanodispersion. Sections were microscopically analyzed using a 20× objective; scale bar: 50 μm. The number of animals in each group was 3.

proteins has not been explored to date. In the present study, we described the obtainment, characterization, and evaluation of a nanodispersion of hexagonal phase for topical delivery of CysA as a model peptide.

The X-ray diffraction and cryo-TEM results demonstrated that the internal structure of the hexagonal (MO/oleic acid/water) phase was preserved after the dispersion of the bulk gel phase in a poloxamer solution by sonication. Even though the sonication process did not influence the liquid crystalline structure of the hexagonal phase, it is well known that the presence of other compounds in the system can influence the packing parameter of the lipid and consequently the liquid crystalline phase formed (5, 34). It has been shown that poloxamer (the dispersion agent) at the polymer/lipid ratio used in the present study (9%) promotes the formation of hexagonal phase dispersion (12). Although a low poloxamer/lipid ratio (<4%) does not allow the formation of a stable dispersion and a high ratio (>9%) prompts the formation of vesicles, poloxamer has been shown not to affect the internal structure of the system (12). This may be explained by the fact that poloxamer, being a large molecule, is excluded from the water channels of the hexagonal phase particles; it is probably adsorbed to the surface of the particles to account for the colloidal stability (11,12). Unlike poloxamer, CysA was demonstrated to concentration-dependently affect the liquid crystalline structure of MO-based systems. CysA at 4% (final concentration) destabilized the structure of the dispersed particles, and a hexagonal structure was no longer observed. This effect of CysA is likely to be related to the observed interaction between monoolein and CysA, which involves the resonance structure of the secondary amides from CysA with the polar headgroup of monoolein (Lopes *et al*., unpublished data). Using CysA at 0.6%, we were able to obtain the hexagonal phase nanodispersion. Thus, 0.6% CysA was selected for further experiments.

As the hexagonal phase nanodispersion had never been used for topical delivery, we first tried to visualize the skin penetration of a fluorescent marker using fluorescence

microscopy. Even though we did not fully characterize whether FITC addition alters the internal liquid crystalline structure of the dispersed particles, it is unlikely to occur based on polarized light microscopy results. Thus, in this experiment we evaluated whether the dispersion formed by two known penetration enhancers (oleic acid and monoolein) would increase the skin penetration of FITC, and hence prove to be a suitable topical delivery system. The application of the dispersion containing FITC on the skin resulted in an increased fluorescence in the viable layers of the skin compared to FITC hydroalcoholic solution.

Next, we evaluated whether the hexagonal phase nanodispersion was able to increase the skin penetration of a large peptide, CysA (MW = 1,202 Da). We observed an increased penetration of CysA in SC and [E + D] *in vitro* 6 h following application of the nanodispersion. No CysA was detected in the receptor phase, which is an advantage of the nanodispersion, because our aim is the topical (not transdermal) delivery of CysA. Like our *in vitro* observations, the *in vivo* skin penetration experiment revealed that incorporation of CysA in the nanodispersion also results in an increase in the skin penetration of the peptide at 6 h postapplication. The skin models used in the *in vitro* and *in vivo* experiments present distinct characteristics, and thus, caution should be taken to compare the results. Mouse skin used in the *in vivo* experiment is more permeable than the porcine skin used in the *in vitro* experiment; thus, skin penetration might be faster in the mouse (35). Additionally, the lack of blood flow in the dermis of the porcine skin *in vitro* may artificially hinder the skin absorption of lipophilic compounds in this water-rich environment (36,37). Even though the skin models used are different, the results obtained *in vivo* confirmed our *in vitro* observation that the nanodispersion enhances skin penetration of CysA. Taken together, these results demonstrate that the hexagonal phase nanodispersion presents the ability to increase the penetration of CysA in the skin compared to a control formulation without affecting the transdermal delivery, and thus, can be a useful strategy to improve the topical delivery of peptides.

In relative terms, a comparison of our *in vitro* results with the results obtained with other colloidal carrier systems reveals that hexagonal phase nanodispersion provided an efficient delivery of CysA, especially to the viable layers of the skin. We observed that 6 h following application of the nanodispersion containing CysA, 7.12 ± 0.94% of the applied dose/cm^2 was delivered to the SC and 3.85 ± 0.96% of the applied dose/cm^2 was delivered to the [E + D], whereas at 12 h postapplication, 13.10 ± 1.65% of the applied dose/cm^2 was delivered to the SC and 5.06 ± 0.78% of the dose/cm^2 was delivered to the [E + D]. In particular, the amount delivered to deep skin layers is higher than that delivered by other methods. Verma and Fahr (20) observed that when CysA was applied in liposomes containing ethanol (10%), 4.079% of the applied dose/cm^2 was delivered to the SC after 6 h, whereas 0.042% of the applied dose/cm^2 was detected in deeper skin layers. Dowton *et al.* (38) studied the influence of vesicle components on CysA penetration in the skin. CysA was incorporated at 0.8–2.2 mg/mL of liposomal dispersion, which was applied in an area of 1.77 cm^2. They reported that, depending on the composition of the carrier, up to 94.3% of the applied dose (after 24 h) may be delivered to the SC, but the amount delivered to deeper skin layers did not exceed 2.1% of the applied dose.

Considering that the applied dose of CysA with the hexagonal phase dispersion was 600 μg, and that ~11% (~7% in the SC and ~4% in E + D) of this dose was found in the permeation area of the skin (which weighs ~0.4 g) at 6 h postapplication in the *in vitro* assay, we estimate that an average skin concentration of CysA of 165 μg/g was achieved using the dispersion. This concentration is 4-fold higher than the concentration of CysA effective to prolong skin allograft survival, as reported by Black *et al.* (39). It should be noted, though, that this analysis is speculative, and that *in vivo* studies in animal models of skin disorders will be necessary to evaluate whether the CysA-bearing nanodispersion would be effective.

Although we did not investigate the mechanism by which the hexagonal phase nanodispersion influences the skin penetration of CysA, some speculation can be made. MO, the main structural lipid of the nanodispersion, is a penetration enhancer that has already been demonstrated to increase skin penetration of peptides and other compounds (1–3,21,40). In a previous study of ours (21), we have shown that, when mixed with propylene glycol, 5–10% of MO promoted not only the skin penetration but also the transdermal delivery of CysA; only at 20–70% MO was the retention of CysA in the skin maximized and its transdermal delivery minimized.

When the nanodispersion was used, an increased concentration of CysA in the skin associated with negligible transdermal delivery was obtained with no more than 8% MO. Hence, the properties of MO do not fully explain the characteristics of the nanodispersion. In addition to MO, the nanodispersion contains oleic acid as a less abundant structural lipid, and oleic acid can also act by itself as a skin penetration enhancer (10). Both MO and oleic acid were shown to be released from a liquid crystalline structure (cubic phase), being available to interact with surface epithelium (2,3). It is of interest that the drug delivery properties of the nanodispersion might also depend on the complex structure of the system. Being a potential intermediary in the membrane fusion process (41), the hexagonal phase may facilitate the fusion of the system particles with SC and deeper skin layers. The hexagonal structure may also improve drug delivery to the skin by protecting the drug from physical and enzymatic degradation (4). Last but not least, the system particles can form a depot in the skin surface and appendages, resulting in a prolonged release of the incorporated compound (42,43). Despite of the many advantages of the hexagonal phase nanodispersion for topical delivery of peptides, it should be pointed out that the therapeutic use of the nanodispersion may be limited by the complexity and the cost of process for its preparation.

The demonstrated ability of the dispersed system to increase the skin penetration of a model peptide suggests a more general use of this system for the topical delivery of several other peptides of dermatological interest. For example, TGF-β and leptin may promote/accelerate wound healing, INF-α may be useful against viral infections, bacitracin and polymixins may be used to treat bacterial infections, and palmytoyl-glycyl–hystidyl–lysine tripeptide may improve overall skin condition by stimulating collagen synthesis

(26,44–47). The application of peptide antigens to the skin is also of interest to the development of vaccines (48,49).

In addition to promoting the delivery of peptides, a viable topical delivery system must produce no or minimal adverse effects. It was thus important to evaluate whether the nanodispersion under investigation would cause skin irritation. By evaluating established endpoints of skin irritation (epidermal thickening, edema, and immunocyte infiltration in dermis), we were able to demonstrate that the daily application of the hexagonal phase nanodispersion for up to 2 days does not cause skin irritation.

A viable delivery system must also display satisfactory long-term stability. Although the stability of the system was not determined in the present study (but is being considered in other ongoing studies in our laboratory), it is noteworthy that at least the structure of the bulk (not dispersed) hexagonal phase is not altered for as long as 5 months after its preparation (Lopes and Bentley, unpublished observations). When it comes to dispersed systems, Esposito *et al.* (16) has shown that organoleptic and morphological aspects of a monoolein-based supramolecular system containing no oleic acid (cubic phase dispersion) do not change for up to 1 year.

CONCLUSION

In conclusion, the present study demonstrates that the nanodispersion of hexagonal phase of monoolein and oleic acid increased the skin penetration of CysA both *in vitro* and *in vivo*, and did not cause skin irritation. Thus, the use of the hexagonal phase nanodispersion is a safe and promising strategy to deliver peptides to the skin.

ACKNOWLEDGMENTS

We thank Dr. Alexandre A. Steiner (St. Joseph's Hospital, Phoenix, AZ, USA) for critical comments on the manuscript, Dr. M. Helena. A. Santana (UNICAMP, Campinas, Brazil) for the light scattering analysis, Dr. Katarina Edwards for Cryo-TEM analysis, Dr. Lia Queiroz do Amaral for helpful discussions, Dr. Colleen M. Brophy (ASU, Tempe, USA) for microscopic facilities, and LNLS (project D11A- SAXS-2461) for the SAXRD measurements. This work was supported by "Coordenação de Aperfeiçoamento de Pessoal de Nível Superior" (CAPES, Brazil), Conselho Nacional de Pesquisa (CNPq, Brazil) and "Fundação de Amparo à Pesquisa do Estado de São Paulo" (FAPESP, Brazil). L.B. Lopes was the recipient of a CNPq fellowship.

REFERENCES

1. M. G. Carr, J. Corish, and O. I. Corrigan. Drug delivery from a liquid crystalline base across Visking and human stratum corneum. *Int. J. Pharm.* **157**:35–42 (1997).
2. J. Lee and I. W. Kellaway. Buccal permeation of [D-Ala, D-Leu] enkephalin from liquid crystalline phases of glyceryl monooleate. *Int. J. Pharm.* **195**:35–38 (2000).
3. J. Lee and I. W. Kellaway. Combined effect of oleic acid and polyethylene glycol 200 on buccal permeation of [D-Ala^2, D-Leu^5] enkephalin from a cubic phase of glyceryl monooleate. *Int. J. Pharm.* **204**:137–144 (2000).
4. J. C. Shah, Y. Sadhale, and D. M. Chilukuri. Cubic phase as drug delivery systems. *Adv. Drug Deliv. Rev.* **47**:229–250 (2001).
5. J. Borné, T. Nylander, and A. Khan. Phase behavior and aggregate formation for the aqueous monoolein system mixed with sodium oleate and oleic acid. *Langmuir* **17**:7742–7751 (2001).
6. M. G. Lara, M. V. L. B. Bentley, and J. H. Collet. *In vitro* drug release mechanism and drug loading studies of cubic phase gels. *Int. J. Pharm.* **293**:241–250 (2005).
7. A. Ganem-Quintanar, D. Quintanar-Guerrero, and P. Buri. Monoolein: a review of the pharmaceutical applications. *Drug Dev. Ind. Pharm.* **26**:809–820 (2000).
8. L. S. Helledi and L. Schubert. Release kinetics of acyclovir from a suspension of acyclovir incorporated in a cubic phase delivery system. *Drug Dev. Ind. Pharm.* **27**:1073–1081 (2001).
9. N. Merclin, J. Bender, E. Sparr, R. H. Guy, H. Ehrsson, and S. Engström. Transdermal delivery from a lipid sponge phase-iontophoretic and passive transport *in vitro* of 5-aminolevulinic acid and its methyl ester. *J. Control. Release* **100**:191–198 (2004).
10. A. C. Williams and B. W. Barry. Penetration enhancer. *Adv. Drug Deliv. Rev.* **56**:603–618 (2004).
11. J. Gustafsson, H. Ljusberg-Wahren, M. Almgren, and K. Larsson. Cubic-lipid–water phase dispersed into submicron particles. *Langmuir* **12**:4611–4613 (1996).
12. J. Gustafsson, H. Ljusberg-Wahren, M. Almgren, and K. Larsson. Submicron particles of reversed lipid phases in water stabilized by a nonionic amphiphilic polymer. *Langmuir* **13**: 6964–6971 (1997).
13. M. Nakano, T. Teshigawara, A. Sugita, W. Leesajakul, A. Taniguchi, T. Kamo, H. Matsuoka, and T. Handa. Dispersions of liquid crystalline phases of the monoolein/oleic acid/pluronic F127 system. *Langmuir* **18**:9283–9288 (2002).
14. K. Larsson. Aqueous dispersions of cubic lipid–water phases. *Curr. Opin. Colloid Interface Sci.* **5**:64–69 (2000).
15. B. Siekmann, H. Bunjes, M. H. J. Koch, and K. Westesen. Preparation and structural investigations of colloidal dispersions prepared from cubic monoglyceride–water phases. *Int. J. Pharm.* **244**:33–43 (2002).
16. E. Esposito, N. Eblovi, S. Rasi, M. Drechsler, G. Di Gregorio, E. Menegatti, and R. Cortesi. Lipid-based supramolecular systems for topical application: a preformulatory study. *AAPS PharmSci.* **5**:1–15 (2003).
17. B. J. Boyd. Characterisation of drug release from cubosomes using the pressure ultrafiltration method. *Int. J. Pharm.* **260**: 239–247 (2003).
18. E. Esposito, R. Cortesi, M. Drechsler, L. Paccamiccio, P. Mariani, C. Contado, E. Stellin, E. Menegatti, F. Bonina, and C. Puglia. Cubosome dispersions as delivery systems for percutaneous administration of indomethacin. *Pharm. Res.* **22**:2163–2173 (2005).
19. J. I. Duncan, S. N. Payne, A. J. Winfield, A. D. Ormerod, and A. W. Thomson. Enhanced percutaneous absorption of a novel topical cyclosporin A formulation and assessment of its immunosuppressive activity. *Br. J. Dermatol.* **123**:631–640 (1990).
20. D. D. Verma and A. Fahr. Synergistic penetration effect of ethanol and phospholipids on the topical delivery of cyclosporin A. *J. Control. Rel.* **97**:55–66 (2004).
21. L. B. Lopes, J. H. Collett, and M. V. L. B. Bentley. Topical delivery of cyclosporin A: an *in vitro* study using monoolein as a penetration enhancer. *Eur. J. Pharm. Biopharm.* **60**:25–30 (2005).
22. G. Kellermann, F. Vicentin, E. Tamura, M. Rocha, H. Tolentino, A. Barbosa, A. Craievich, and I. Torriani. The small-angle X-ray scattering beamline of the Brazilian Synchrotron Light Laboratory. *J. Appl. Crystallogr.* **30**:880–883 (1997).
23. A. F. Craievich. Synchrotron SAXS studies of nanostructured materials and colloidal solutions. A review. *Mater. Res.* **5**:1–11 (2002).
24. J. R. Bellare, H. T. Davis, L. E. Scrie, and Y. Talmon. Controlled environment vitrification system: an improved sample preparation technique. *J. Electron Microsc. Tech.* **10**:87–111 (1988).
25. L. B. Lopes, C. M. Brophy, E. Furnish, C. R. Flynn, O. Sparks, P. Komalavilas, L. Joshi, A. Panitch, and M. V. Bentley. Comparative study of the skin penetration of protein transduction domains and a conjugated peptide. *Pharm. Res.* **22**:750–757 (2005).

26. M. Foldvari, M. E. Baca-Estrada, Z. He, J. Hu, S. Attah-Poku, and M. King. Dermal and transdermal delivery of protein pharmaceuticals: lipid-based delivery systems for interferon-α. *Biotechnol. Appl. Biochem.* **30**:129–137 (1999).
27. E. Touitou, N. Dayan, L. Bergelson, B. Godin, and M. Eliaz. Ethosomes—novel vesicular carriers for enhanced delivery: characterization and skin penetration properties. *J. Control. Rel.* **65**:403–418 (2000).
28. G. R. Pereira, J. H. Collett, S. B. Garcia, J. A. Thomazini, and M. V. L. B. Bentley. Glycerol monooleate/solvents systems for progesterone transdermal delivery: *in vitro* permeation and microscopic studies. *Braz. J. Pharm. Sci.* **38**:55–62 (2002).
29. J. Guo, Q. Ping, G. Sun, and C. Jiao. Lecithin vesicular carriers for transdermal delivery of cyclosporin A. *Int. J. Pharm.* **194**:201–207 (2000).
30. A. Sintov, A. Ze'evi, R. Uzan, and A. Nyska. Influence of pharmaceutical gel vehicles containing oleic acid/sodium oleate combinations on hairless mouse skin, a histological evaluation. *Eur. J. Pharm. Biopharm.* **47**:299–303 (1999).
31. R. Alvarez-Román, A. Naik, Y. N. Kalia, H. Fessi, and R. H. Guy. Visualization of skin penetration using confocal laser scanning microscopy. *Eur. J. Pharm. Biopharm.* **58**:301–316 (2004).
32. H. Chung, J. Kim, J. Y. Um, I. C. Kwon, and S. Y. Jeong. Self-assembled "nanocubicle" as a carrier for peroral insulin delivery. *Diabetologia* **45**:448–451 (2002).
33. J. Y. Um, H. Chung, K. S. Kim, I. C. Kwon, and S. Y. Jeong. *In vitro* cellular interaction and absorption of dispersed cubic particles. *Int. J. Pharm.* **253**:71–80 (2003).
34. F. Caboi, G. S. Amico, P. Pitzalis, M. Monduzzi, T. Nylander, and K. Larsson. Addition of hydrophilic and lipophilic compound of biological relevance to the monoolein/water system. I—Phase behavior. *Chem. Phys. Lipids* **109**:47–62 (2001).
35. K. Moser, K. Kriwet, A. Naik, Y. N. Kalia, and R. H. Guy. Passive skin penetration enhancement and its quantification *in vitro*. *Eur. J. Pharm. Bipharm.* **82**:103–112 (2001).
36. K. Moser, K. Kriwet, A. Naik, Y. N. Kalia, and R. H. Guy. Passive skin penetration enhancement and its quantification *in vitro*. *Eur. J. Pharm. Bipharm.* **82**:103–112 (2001).
36. W. G. Reinfarah, G. S. Hawkins, and M. S. Kurtz. Percutaneous penetration and skin retention of topically applied compounds: an *in vitro–in vivo* study. *J. Pharm. Sci.* **80**:526–531 (1991).
38. S. M. Dowton, C. Hu, C. Ramachandram, D. H. F. Wallach, and N. Weiner. Influence of liposomal composition on topical delivery of encapsulated cyclosporin A. I. An *in vitro* study using hairless mouse skin. *STP Pharma Sci.* **3**:404–407 (1993).
39. K. S. Black, D. K. Nguyen, C. M. Proctor, M. P. Patel, and C. W. Hewitt. Site-specific suppression of cell-mediated immunity by cyclosporine. *J. Invest. Dermatol.* **94**:644–648 (1990).
40. T. Ogiso, M. Ywaki, and T. Paku. Effect of various enhancers on transdermal penetration of indomethacin and urea and relationship between penetration parameters and enhancement factors. *J. Pharm. Sci.* **84**:482–488 (1995).
41. G. Cevc and H. Richardsen. Lipid vesicles and membrane fusion. *Adv. Drug Deliv. Rev.* **38**:207–232 (1999).
42. C. Cevc, G. Blume, A. Schatzelein, D. Gebauer, and A. Paul. The skin: a pathway for systemic treatment with patches and lipid-based agent carriers. *Adv. Drug Deliv. Rev.* **18**:349–378 (1996).
43. C. Cevc. Lipid vesicles and other colloids as drug carriers on the skin. *Adv. Drug Deliv. Rev.* **56**:675–711 (2004).
44. T. F. Zioncheck, S. A. Chen, L. Richardson, M. Mora-Worms, C. Lucas, D. Lewis, J. D. Green, and J. Mordenti. Pharmacokinetics and tissue distribution of recombinant human transforming growth factor beta 1 after topical and intravenous administration in male rats. *Pharm. Res.* **11**:213–220 (1994).
45. S. Frank, B. Stallmeyer, H. Kampfer, N. Kolbe, and J. Pfeilschifter. Leptin enhances wound re-epithelization and constitutes a direct function of leptin in skin repair. *J. Clin. Invest.* **106**:501–509 (2000).
46. K. Lintner and O. Peschard. Biologically active peptides: from a laboratory bench curiosity to function skin care product. *Int. J. Cosmet. Sci.* **22**:207–218 (2000).
47. C. T. Spann, S. C. Taylor, and J. M. Weinberg. Topical antimicrobial agents in dermatology. *Dis. Mon.* **50**:407–421 (2004).
48. C. D. Partidos, A. S. Beignon, F. Mawas, G. Belliard, J. P. Briand, and S. Muller. Immunity under the skin: potential application for topical delivery of vaccines. *Vaccine* **21**:776–780 (2003).
49. C. D. Partidos, E. Moreau, O. Chaloin, M. Tunis, J. P. Briand, C. Desgranges, and S. Muller. A synthetic HIV-1 Tat protein breaches the skin barrier and elicits Tat-neutralizing antibodies and cellular immunity. *Eur. J. Immunol.* **34**:3723–3731 (2004).